

AD-A056 466

ARMY MATERIALS AND MECHANICS RESEARCH CENTER WATERTO--ETC F/G 17/9
RADAR ABSORPTIVE MATERIAL FORM INDUSTRIAL EFFLUENT, (U)
JUN 78 J W MCCAULEY, B M HALPIN, S D EITELMAN

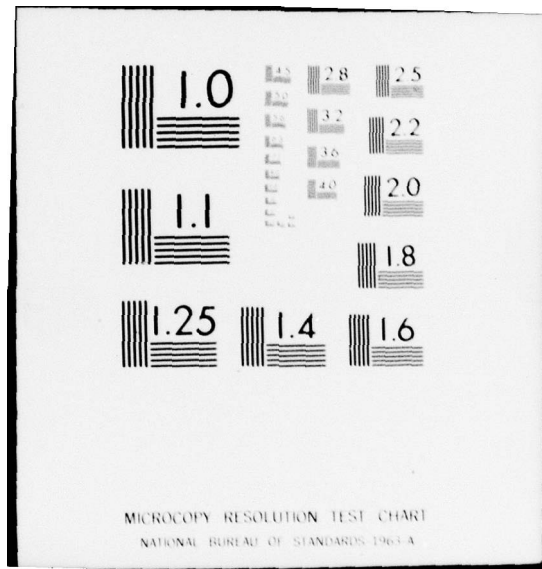
UNCLASSIFIED

NL

1 of 1
AD
A056 466



END
DATE
FILMED
8 -78
DDC



MICROCOPY RESOLUTION TEST CHART
NATIONAL BUREAU OF STANDARDS-1963-A

AD A 056466

LEVEL II



*McCAULEY, HALPIN, EITELMAN,
and HYNES

14 James W./McCauley, Bernard M./Halpin, Jr.,
Stephen D./Eitelman Thomas V./Hynes

6 RADAR ABSORPTIVE MATERIAL FORM INDUSTRIAL EFFLUENT.

DDC
RECEIVED
JUL 12 1978

11 JUN 1978

12 15p.

*JAMES W. McCAULEY, PhD
BERNARD M. HALPIN, JR., PhD
ARMY MATERIALS AND MECHANICS RESEARCH CENTER, WATERTOWN, MA 02172
STEPHEN D. EITELMAN, MR.
U.S. ARMY MATERIEL DEVELOPMENT AND READINESS COMMAND
ALEXANDRIA, VA 22333
THOMAS V. HYNES, PhD
ARMY MATERIALS AND MECHANICS RESEARCH CENTER, WATERTOWN, MA 02172

D
Handwritten initials

AD No. _____
DDC FILE COPY,

I. INTRODUCTION

Recent innovative work (1,2) by the Nippon Electric Co. (NEC) Tokyo, Japan, on a ferrite precipitation method for removing heavy metal ions from industrial waste water and the subsequent potential use of this material (ferrite sludge) as a cheap microwave absorber has stimulated interest in the possible United States military applications of this concept. An important factor in this consideration is that the cost of the material is projected as significantly less than currently available ferrite material. This report describes the results of this program: a characterization and fabrication phase carried out at the Army Materials and Mechanics Research Center, Watertown, Massachusetts, and a testing phase carried out at the U.S. Army Electronic Proving Ground, Fort Huachuca, Arizona.

II. MAGNETIC DIELECTRIC RADAR SIGNATURE REDUCTION

One way of reducing radar signatures of highly reflective materials is by the use of radar-absorbing coating materials. Magnetic dielectrics (ferrites) are a family of materials that can absorb microwaves by the lossy interaction of the electric and magnetic vectors of an electromagnetic wave with the material.

403 105
78 06 12 007

DISTRIBUTION STATEMENT A
Approved for public release;
Distribution Unlimited

Handwritten initials

*McCAULEY, HALPIN, EITELMAN
and HYNES

When an electromagnetic wave strikes an object there is generally a reflection because of a discontinuity in electrical properties between the medium the wave is travelling and the object it strikes. One can show the following: an electromagnetic wave of amplitude E_0 travelling in free space (μ [the magnetic permeability] = μ_0 , and ϵ [the electrical permittivity] = ϵ_0) and striking a plane surface A ($\mu_A = \mu_A' + i\mu_A''$ and $\epsilon_A = \epsilon_A' + i\epsilon_A''$, where $\mu_A' \gg \mu_A''$ and $\epsilon_A' \gg \epsilon_A''$) will have a reflection approximately $[1 - [(\mu_A'/\epsilon_A') (\epsilon_0/\mu_0)]^{1/2}]$ in magnitude. If $\mu_A'/\epsilon_A' = \mu_0/\epsilon_0$, there will be no reflection. The wave will be attenuated in the material by a factor $\exp(-\mu_A'' \omega [\mu_A'/\epsilon_A']^{-1/2} \ell)$ where $\omega = 2\pi$ frequency and ℓ = the depth in the material. Thus by properly choosing the permeability, dielectric constant, depth, and loss factors, normal incident waves can be absorbed in the material. Unfortunately, however, all factors vary with frequency and this factor must be taken into consideration in the exact calculations. In this investigation, microwave attenuation and concomitant radar signature reductions have been achieved by an increase in the magnetic permeability and magnetic losses of a dielectric material.

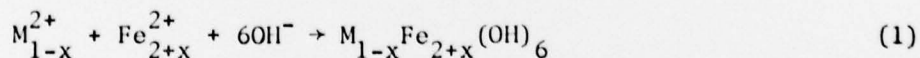
III. DESCRIPTION OF FERRITE PRECIPITATION PROCESS

Stimulated by more stringent pollution control requirements in Japan, the NEC is investigating the use of a ferrite precipitation process to remove heavy metals from their industrial waste water (1). They have two motives for exploring this unique idea: (1) purification of industrial waste water and (2) simultaneous formation of significantly cheaper ferrite raw material for possible commercial use. Potential uses envisioned by them include prevention of double TV images (ghosts) by using ferrite coatings on buildings and also elimination of ground reflections near radar receivers by coating the ground.

Standard industrial practice (3) used in the production of ferrite materials consists of elaborate mixing, pressing, and controlled heat treatments of carefully weighed, mechanically pulverized, and mixed ceramic oxide powders. The novel technique being used by NEC is a wet chemical reaction process referred to as coprecipitation. Essentially, divalent iron and other metal ions are hydrolyzed in a basic solution and then oxidized into the ferrite spinel structure (2).

The two steps can be formularized as follows:

Hydrolysis:

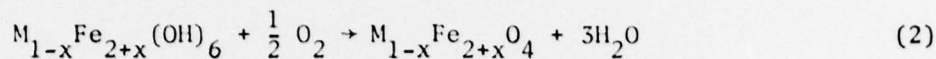


SESSION NO.	White Section Buff Section
ANNOUNCES	
CLASSIFICATION	Per Basic rpt.
EXTENSION/AVAILABILITY CODES	
SEC. AVAIL. and/or SPECIAL	
	A

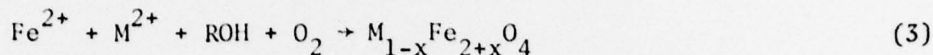
78 06 12 007

*McCAULEY, HALPIN, EITELMAN
and HYNES

Warm Aeration:



or more simply as



where R = alkali or alkali earth cation (ex. NaOH).

In summary, the ferrite sludge coprecipitation process is schematically illustrated in Figure 1.

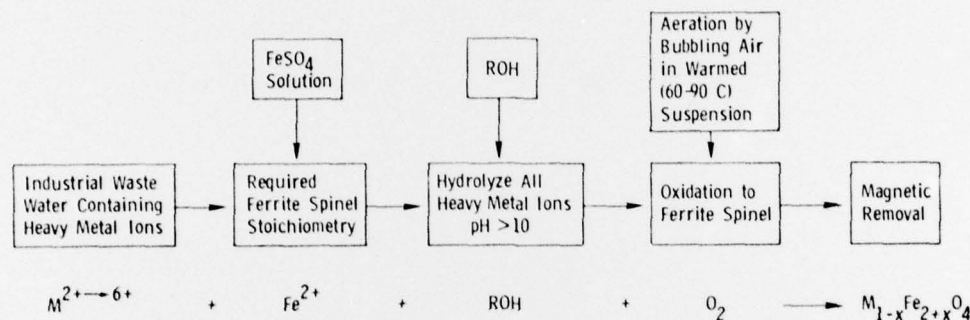


Figure 1. Schematic flow chart for the production and removal of ferrite sludge by the coprecipitation process.

Experimental data demonstrate that the heavy metal removal technique is successful. Table 1 lists various heavy metal ions in the industrial waste water before and after the coprecipitation treatment (1).

IV. CHARACTERIZATION OF FERRITE SLUDGE

Two separate batches of sludge, nominally referred to as the 5-kg and 50-kg batches, were obtained from NEC. They were brown to dark brown in color and had a mud-like consistency. Figure 2 illustrates both the as-received material and also the dried, ball-milled, and sieved (-325 mesh) powder.

Table 1. HEAVY METAL ION CONCENTRATIONS IN INDUSTRIAL WASTE WATER BEFORE AND AFTER FERRITE SLUDGE COPRECIPITATION TREATMENT.

Heavy Metal Ion	Concentration in Waste Water (ppm)	
	Before Treatment	After Treatment
Cu	9,500	< 0.5
Ni	20,000	< 0.5
Sn	4,000	< 10
Pb	6,800	< 0.1
Cr ⁶⁺	2,000	< 0.1
Cd	1,800	< 0.1
Fe	over 1%	< 1.0
Hq	3,000	ND*

*Nondetectable

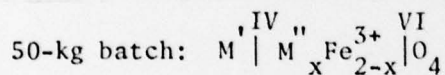
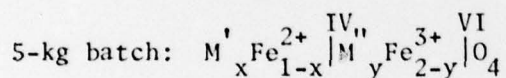
*McCAULEY, HALPIN, EITELMAN
and HYNES



Figure 2. Ferrite sludge.

The as-received sludge contains appreciable amounts of water and must be thoroughly dried prior to further use. Table 2 lists the water content and approximate chemistry of the two batches which are quite different in composition, the 5-kg batch being iron-rich and the 50-kg batch being iron-poor.

Hypothetical chemical-structural formulas for these ferrite spinels are as follows (4,5):



M', M'' = heavy metal ions,

IV, VI = tetrahedral and octahedral coordination, respectively.

There are eight formula units in the ferrite spinel unit cell, yielding the following actual chemical formula: $M'_8 M''_{8x} \text{Fe}_{16-8x} \text{O}_{32}$.

Hence, there are at least $M'_8 + M''_{8x}$ crystallographic sites in the unit cell for the removed heavy metal ions.

Figure 3 is a diagrammatic representation of the actual powder diffraction patterns using filtered $\text{CrK}\alpha$ radiation. The 5-kg batch is 100% ferrite with a LiFe_5O_8 (ferrite)-like structure. The 50-kg sludge is a relatively impure ferrite sample containing several nonferrite phases. Roughly 60% of the mixture is a ferrite similar to LiFe_5O_8 ,

Table 2. CHEMISTRY OF AS-RECEIVED FERRITE SLUDGE

Element	Weight Percent in Batches	
	5 kg	50 kg
H_2O^*	45.0	43.9
Fe [†]	65.7	49.2
Mn [‡]	0.5-1	1
Mg	.5	1
Al	.1-0.5	1
Ni	.5	1
Si	.5	1-10
Pb	.1-0.5	0.5-1
Sn	.05	.5
Zn	.1	.5-1
Cr	.01	.5
Ca	.1	.5
Cd	.5	.5
Cu	.05	.05-0.1
Mo	.05-0.1	.05-0.1
Ti	.01-0.05	.1-0.5
Zr	.05	.05
Ba	.05	.05

*Loss on drying at 105 C.

†Quantitative analysis for Fe by wet chemistry

‡All the remaining analysis are semiquantitative emission spectroscopic results reported in weight percent

*McCAULEY, HALPIN, EITELMAN
and HYNES

3% is $\text{Fe}(\text{OH})_3$, 6% is ZnCr_2O_4 (spinel), 11% is NiO , and the last 20% consists of FeCl_3 , CaSnO_4 , and CaFeO_7 (ferrite). It is also possible that a significant percentage of both batches contain X-ray amorphous phases and therefore do not appear in the diffraction patterns.

Table 3 lists the physical powder characteristics of the two batches. Figure 4 illustrates a high magnification view of the 5-kg powder, showing its very fine grain size. The 5-kg batch is a higher density, larger grain size material than the 50-kg material. Ideal densities for ferrites of similar chemistry as reported here are about 5.0 g/cc, close to the 5-kg material, but significantly different than the 50-kg material. All these data indicate that the 5-kg powder more

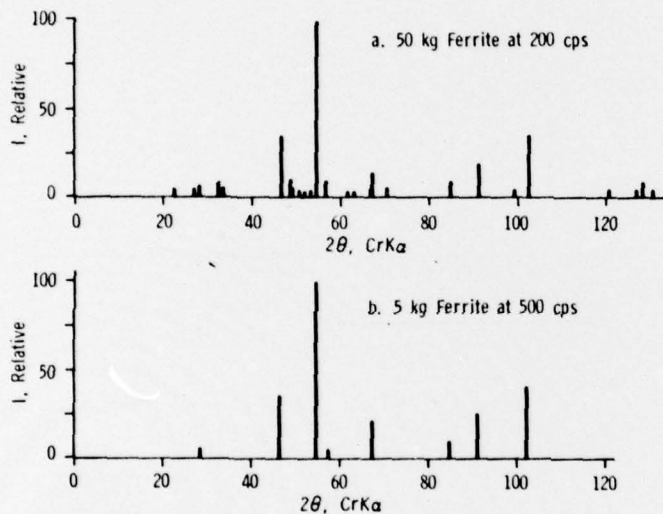


Figure 3. X-ray powder diffraction patterns ($\text{CrK}\alpha$) of two dried, ball-milled, and sieved (-325) ferrite sludge powders; $\text{CrK}\alpha$ radiation.

Table 3. POWDER CHARACTERISTICS OF FERRITE SLUDGE

Drying Conditions: 150 C, 24 hr						
Type kg	Heat Treatment			Surface Area*	Equivalent Spher. Diam.†	ρ_0 ‡
	T°C	t(hr)	Atm	m^2/g	μm	g/cc
5	-	-	-	20.83	0.058	4.88
5	480	24	Air	16.12	0.075	-
5	480	72	Air	14.26	0.084	-
50	-	-	-	29.97	0.040	3.81
50	400	26	Air	23.77	0.050	-
50	400	136	Air	23.11	0.052	-

*By a BET technique

†Equivalent spherical diameter assuming a density of 5.0 g/cc

‡Measured density by a helium-air pycnometer method

*McCAULEY, HALPIN, EITELMAN
and HYNES



Figure 4. SEM photomicrograph of fracture surface of ferrite sludge powder cold isostatically pressed at 20,000 psi and heat treated for 24 hr at 200 C.

nearly represents a ferrite material, whereas the 50-kg material is a very impure ferrite powder, suggesting that the NEC process will not yield identical material. However, the ferrite sludge in both cases is a magnetic ferrite, and no heat treatment is required to form a ferrite phase as in conventional ferrite manufacturing processes. Further, there seems to be a direct correlation between the iron content and the ferrite content of the two batches. This implies that enough FeSO_4 must be added to coprecipitate all the heavy metals in a ferrite phase, otherwise the hydrolysis and warm aeration will produce other nonferrite material.

V. FABRICATION PROCEDURE

Three processing routes were analyzed for use in the production of the large 12" × 12" testable sample tiles:

- a. pressed powder, no heat treatment,
- b. sintered powder, and
- c. organic matrix composite.

Prior work by the NEC implied that either a or b was sufficient for wave guide (VSWR) microwave absorption measurements on small samples (6-8). However, because of our remote test location and large sample requirements for radar absorption measurements only methods b and c were considered practical. In order to decide between these procedures a preliminary thermal analysis and sintering study was carried out on the two batches.

*McCAULEY, HALPIN, EITELMAN
and HYNES

a. Thermal Analysis

Initial sintering runs clearly demonstrated a complex sequence of reactions and densification characteristics, the major problem being the oxidation of the ferrite to the nonmagnetic $\alpha\text{-Fe}_2\text{O}_3$ (hematite) phase. The reaction can be simplified as follows:

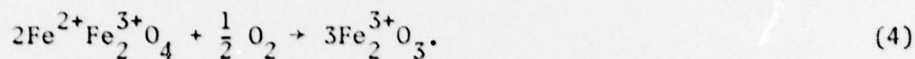


Figure 5 illustrates the thermogravimetric analysis (TGA) curves for the two batches and Figure 6 shows the differential thermal analysis (DTA) traces of heat-treated and untreated samples. Apparently, because of excessive volatilization of nonferrite metal oxide phases, the TGA curves show weight losses and not weight gains as would be expected for reaction (Eq. 4). However, the DTA curves clearly show the $\alpha\text{-Fe}_2\text{O}_3$ reaction at about 604 C in the 5-kg material (Figure 6a) and roughly 340 C in the 50-kg material (Figure 6b). This was confirmed by X-ray diffraction analysis of resultant products. In an attempt to stabilize the ferrite spinel structure, extended heat treatments were carried out below the transformation temperature. The DTA curves for these heat-treated samples (Figures 6c and 6d), however, again show the $\alpha\text{-Fe}_2\text{O}_3$ transformation. Clearly, heat treatment in air above the

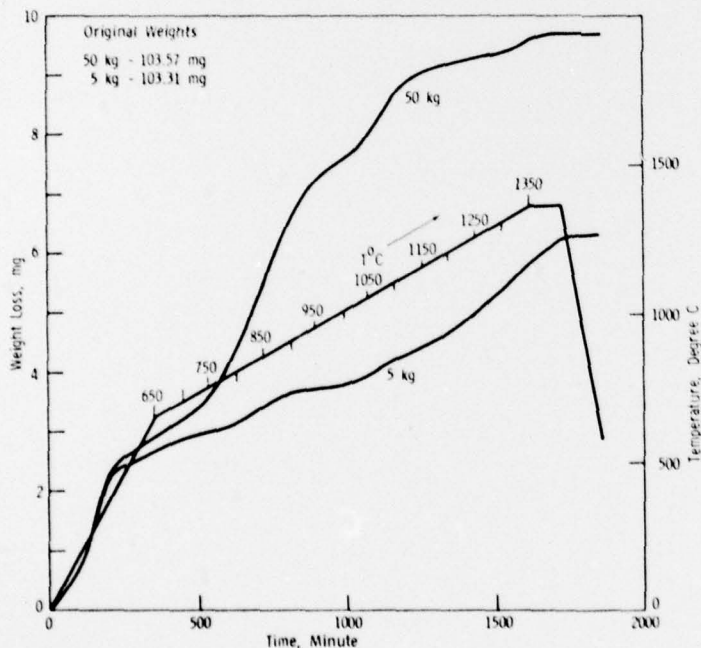


Figure 5. Thermogravimetric analysis traces of predried and pressed ferrite sludge powder.

*McCAULEY, HALPIN, EITELMAN
and HYNES

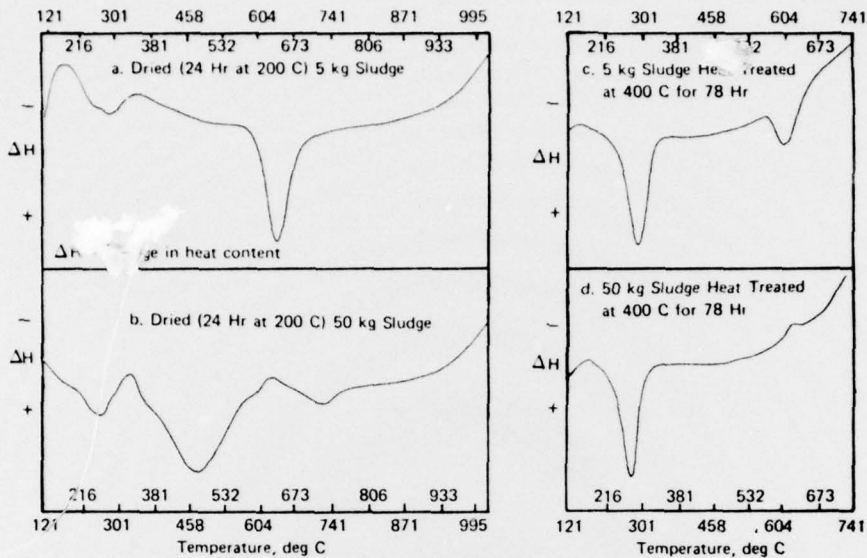


Figure 6. Differential thermal analysis heating curves of ferrite sludge powders - all heated in air.

α -Fe₂O₃ transformation temperature always results in an α -Fe₂O₃ product which is unacceptable. One additional DTA experiment using flowing argon instead of air confirmed this deduction.

b. Sintering Studies

Preliminary sintering work was also carried out with a summary of the data plotted on Figure 7, showing the variation of observed densities as a function of temperature. The data simply reflects the oxidation of the ferrite sludge to α -Fe₂O₃ and its subsequent densification. All samples were isostatically cold pressed at 20,000 psi prior to heat treatment. Scanning electron microscope (SEM) photomicrographs of fracture surfaces of runs labeled 18, 23, and 24 in Figure 7 are presented in Figure 8. As can be seen, sintering in flowing air results in a completely α -Fe₂O₃ body (Figure 8b), whereas sintering in argon or a limited amount of air results in a sintered ceramic containing ferrite (Figure 8a and 8c). Figure 9 shows the microstructural details of the precipitation of α -Fe₂O₃ from a ferrite matrix. This sample was dried at 200 C for 24 hours and then heat treated at 1200 C for 24 hours in air. All these data indicate that the production of large fully-sintered ferrite ceramic tiles must be preceded by an in-depth atmosphere-controlled sintering study, which was deemed prohibitively expensive as a processing procedure.

*McCAULEY, HALPIN, EITELMAN
and HYNES

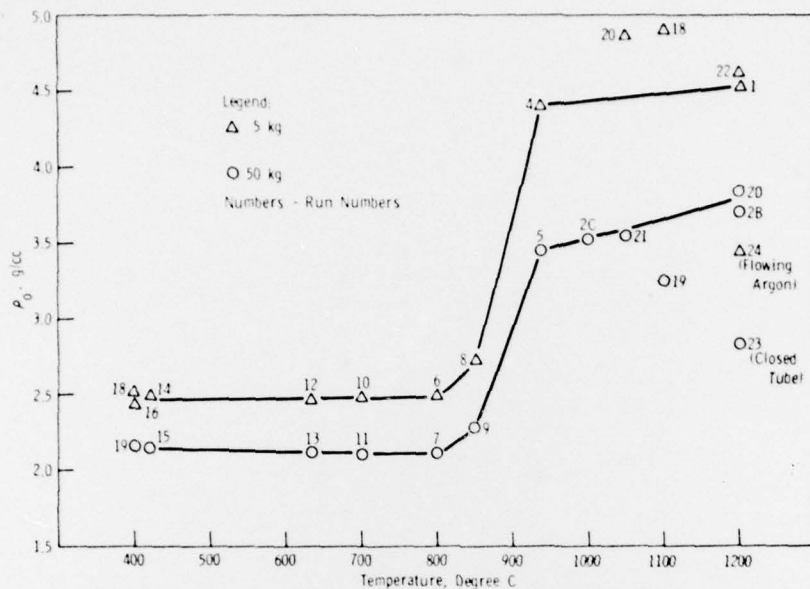
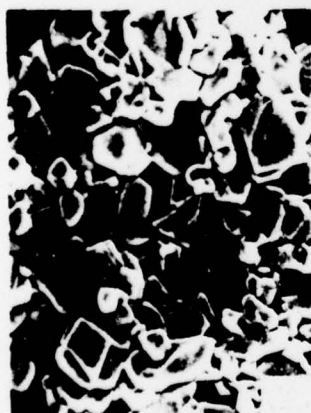
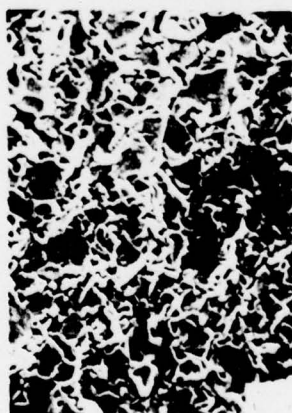


Figure 7. Variation of observed density of heat-treated ferrite sludge powder.



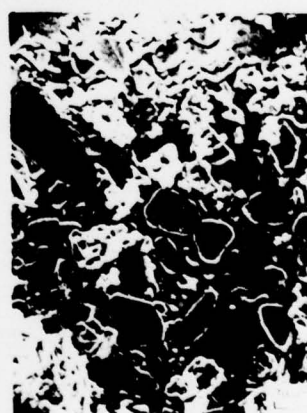
a. 100% Ferrite; Calcined in Air at 487 C for 22 Hr, Sintered at 1200 C for 4 Hr in Flowing Argon

(Run 24)



b. 100% α -Fe₂O₃; Calcined in Air at 400 C for 78 Hr, Sintered at 1100 C for 40 Hr in Air

(Run 18)



c. 22% Ferrite, 78% α -Fe₂O₃; Calcined in Air at 400 C for 48 Hr, Sintered at 1200 C for 4 Hr in Closed Muffle Tube

(Run 23)

Figure 8. SEM photomicrographs of representative fracture surface microstructures of heat-treated ferrite sludge powders.

*McCAULEY, HALPIN, EITELMAN
and HYNES

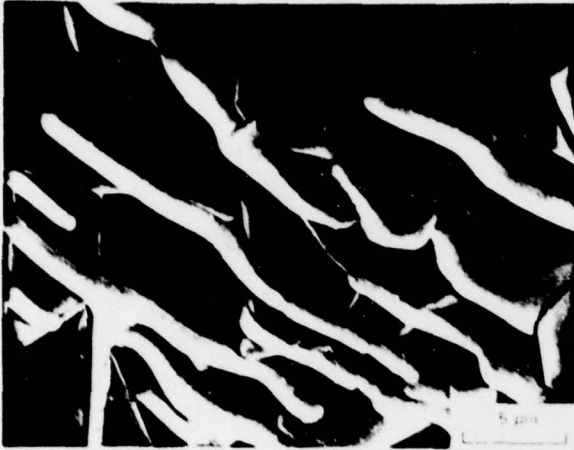


Figure 9. SEM photomicrograph of fracture surface of ferrite sludge heat treated at 1200 C in air for 24 hours. Microstructure of precipitation of lenticular $\alpha\text{-Fe}_2\text{O}_3$ from ferrite matrix.

c. Feasibility of Organic Matrix

It was very quickly demonstrated that at least 50 wt% ferrite powder (-325 mesh) could easily be incorporated into an EPON 828/Z curing agent (100 parts/20 parts) epoxy resin matrix. The powder was not rejected by the resin and formed a homogeneous ferrite/resin composite material and did not lose its magnetic properties.

VI. PRODUCTION OF FERRITE/RESIN TILES

A special mold was constructed to form, de-gas, and cure the ferrite/resin composite. Additionally, it was designed to have a 1/16" overhang of resin over the Al backup plate to prevent direct exposure of the Al plate to the microwave signals, even in a slightly tilted situation. The following is a summary of the final fabrication process.

- a. Dry at 150 C and ball mill for at least 24 hours.
- b. Sieve all powder through -325 mesh screen.
- c. Mechanically blend 50 wt% ferrite powder in an EPON 828/Z curing agent resin mixture.
- d. Casting procedures:
 - (1) Self-bonding
 - (a) De-gas ferrite/resin mixture.
 - (b) Cure 2 hr at 175 F, 2 hr at 300 F, directly to Al backup plate.

*McCAULEY, HALPIN, EITELMAN
and HYNES

(2) Two-step process

- (a) De-gas ferrite/resin mixture.
- (b) Cure 4 hr at 175 F using a mold release on Al backup plate.
- (c) Bond to Al backup plate using a two-part Epoxy Adhesive 907.
- e. Grind ferrite/epoxy surface to final required thickness dimension.

Four composite plates were fabricated and described in Table 4. Samples FP-1 through FP-4 were all bonded to 12" x 12" x 5/16" Al plates; the ferrite/resin composites measured 12-1/8" x 12-1/8". Side views of these test panels can be seen in Figure 10.



Table 4. DESCRIPTION OF FERRITE/RESIN COMPOSITE PLATES

Sample	Ferrite	Resin Thickness	Process
FP-1	Undoped	1/8"	1 step
FP-2	50 kq-50 Wt%	1/8"	1 step
FP-3	50 kq-50 Wt%	3/8"	2 step
FP-4	5 kq-50 Wt%	1/8"	2 step
FP-5	Blank Al Plate		

Figure 10. Photograph of four test tiles and standard Al plate - side view.

*McCAULEY, HALPIN, EITELMAN
and HYNES

VII. MICROWAVE ABSORPTION TESTS

The microwave absorption tests were carried out by Captain J. Newton, Mr. K. Hakes, Mr. W. Krotzer, and Warrant Officer G. Van Horn at the Electromagnetic Interference Laboratory, Black Tail Canyon Test Facility, U.S. Army Electronic Proving Ground, Fort Huachuca, Arizona. Figure 11 is a drawing of the actual arrangement of the test panel, receiving antenna, and transmitting horn used in this experiment. After several unsatisfactory series of measurements using either a wood or lucite test panel holder, a target holder consisting of a styrofoam block with a recess cut to hold the test panels was selected for the final measurements.

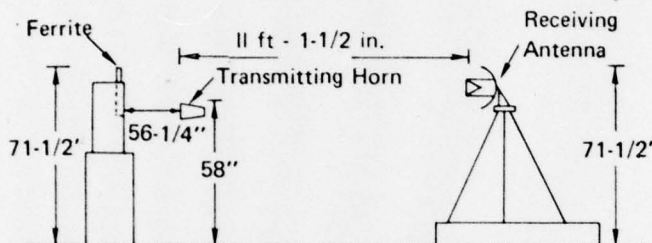


Figure 11. Physical arrangement of microwave test equipment and test plate in Fort Huachuca anechoic chamber.

Average Δ dB (difference between the standard uncoated Al plate and ferrite/resin coated plates) and equivalent percent absorption for the various test panels are plotted against frequency in Figure 12. Also plotted on the figure are the common radar bands of interest. All the microwave measurements were repeatable within 1.5 dB. There is significant attenuation of the microwave signals by the 50-kg 3/8"-thick ferrite/resin composite in two regions: about 5 dB absorption (68%) in the 3 to 4.5 GHz region and over 6 dB absorption (75%) in the 10 to 13 GHz J-band region. There also seems to be small absorptions at about 7 and 8 GHz. All three ferrite-treated resins show similar effects, the 3/8"-thick composite with the impure 50-kg ferrite exhibiting the most pronounced. However, from 4 to 8 GHz a small enhancement in attenuation of the 5-kg (pure) ferrite over the 50-kg (impure) ferrite did seem to occur. In general, there was a negligible dependence of absorption on the purity of the ferrite powder, suggesting that the Fe content of the sludge could be significantly reduced without appreciably affecting the radar absorption properties.

*McCAULEY, HALPIN, EITELMAN
and HYNES

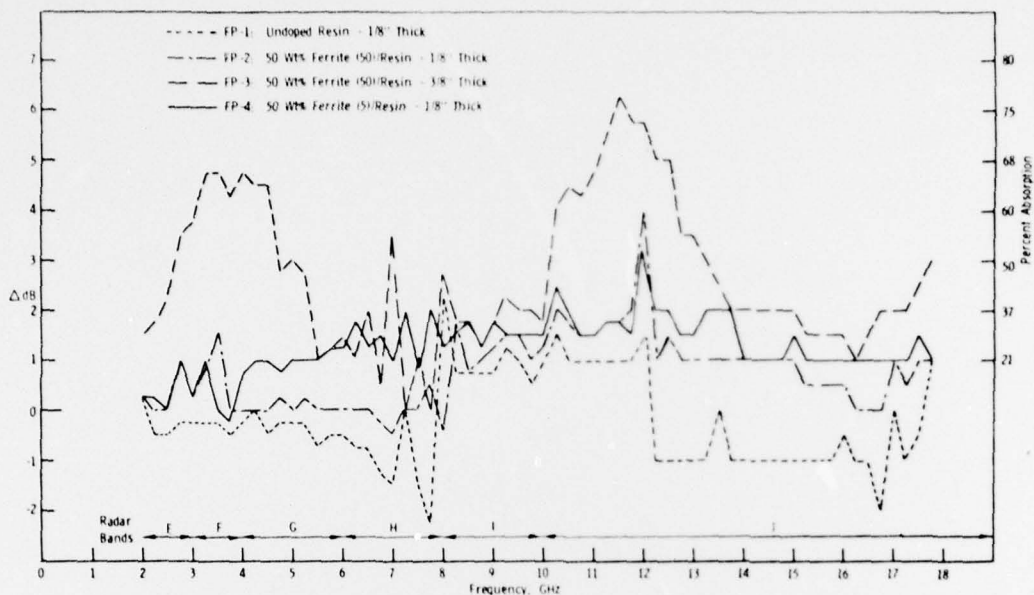


Figure 12. Graphical results of microwave absorption tests of ferrite/resin composites; difference in amplitude from Al plate (Δ dB) plotted against frequency (GHz).

VIII. SUMMARY AND CONCLUSIONS

A comprehensive study has been carried out to evaluate the microwave absorption potential of a ferrite sludge derived by a coprecipitation treatment of industrial waste water. Full characterization of two different batches of sludge showed quite different chemistries, especially in the amount of iron content; one was iron-rich, the other iron-poor, differing by about 15% to 16% Fe. The iron-rich ferrite was determined to be 100% ferrite spinel, whereas the iron-poor ferrite was only 60% ferrite. The powders have an extremely fine grain size with a surface area of 20 to 30 m^2/g , indicative of an average equivalent spherical diameter of about 0.05 μm . Careful thermal analysis and sintering studies clearly demonstrated that only carefully controlled atmospheres can be used to sinter the ferrite sludge powder into a mechanically coherent ferrite ceramic. The major problem is the oxidation of the ferrite to the nonmagnetic α - Fe_2O_3 (hematite) phase at relatively low temperatures. Because of these constraints a ferrite/resin (EPON 828/Z) composite system was selected as the most appropriate material configuration for the microwave absorption evaluation of the sludge. Microwave testing of four test panels in the Fort Huachuca anechoic chamber demonstrated significant attenuation of the microwave signals by a 3/8"-thick ferrite/resin composite in two

*McCAULEY, HALPIN, EITELMAN
and HYNES

regions: 3 to 4.5 GHz (68%) and 10 to 13 GHz (75%). There seemed to be no significant difference in results using either the iron-rich or iron-poor ferrite sludge material, showing that significantly less iron could be used in the ferrite coprecipitation waste water treatment process.

The data obtained in our investigation and the unconfirmed results of NEC strongly suggest that the ferrite sludge concept could prove to be an important new method of inexpensively reducing radar signatures, by either a coating technique or smoke generation, while stimulating the ecologically important purification of industrial waste water. Also the possibility exists that the fundamental concept confirmed in this program could be further optimized. Moreover, it is our conclusion that the fabrication of massive fully sintered radar-absorbing ceramic ferrites would prove prohibitively expensive and unjustifiable from a practical point of view. Instead, the organic-based matrix concept seems to be the most practical and feasible at this point, as well as the use of the ferrite powder in camouflage smokes.

IX. ACKNOWLEDGMENTS

The authors wish to acknowledge the assistance of many people in carrying out this project: Dr. D. Messier (TGA) and Messrs. P. Wong, A. Connolly (SEM), T. Sheridan (X-ray), and G. Bluteau (chemical analysis) for their assistance in the initial stages of the characterization effort, and also to Messrs. D. Corkum, N. Corbin, K. Lucas, A. Reppucci, and C. MacQueen for their invaluable help in the fabrication and sintering studies. We also would like to gratefully acknowledge the appreciated cooperation of the following people at Fort Huachuca who carried out the tests: Captain J. Newton, Mr. K. Hakes, Mr. W. Krotzer, and Warrant Officer G. Van Horn.

*McCAULEY, HALPIN, EITELMAN
and HYNES

REFERENCES

1. ASAI, G. N. *Research Planned by Nippon Electric Co., Ltd., on the Prevention of Electromagnetic Wave Reflection by the Use of Ferrite Sludge*. U.S. Army Foreign Science and Technology Center, Report 2-253-0111-74, February 1974.
2. TAKADA, T., and KIYAMA, M. *Preparation of Ferrites by Wet Method: Ferrites* in Proceedings of the International Conference, ed., Y. Hoshino, S. Iida, and M. Sugimoto, University Park Press, Tokyo, Japan, 1970.
3. PAULUS, M. *Preparation Conditions of the Ferrites* in Preparative Methods in Solid State Chemistry, ed., P. Hagenmuller, Academic Press, New York, 1972, p. 487-531.
4. GRAY, T. J. *Oxide Spinel* in High Temperature Oxides - Part IV, Refractory Glasses, Glass-Ceramics, and Ceramics, ed., A. M. Alper, Academic Press, New York, 1971, p. 77-107.
5. BLASSE, G. *Crystal Chemistry and Some Magnetic Properties of Mixed Metal Oxides with Spinel Structure*. Philips Research Reports Supplements, no. 3, 1964, 139 pages.
6. ASAI, G. N. *Research on Treatment and Properties of Ferrite Sludge for Microwave Absorption*. U.S. Army Foreign Science and Technology Center, Report 2-253-0593-75, 12 August 1975, (FOUO).
7. AKASHI, T., SUGANO, I., OKUDA, T., and TSUJI, T. *Sintering of Coprecipitated Manganese Zinc Ferrite Powder: Ferrites* in Proceedings of the International Conference, ed., Y. Hoshino, S. Iida, and M. Sugimoto, University Park Press, Tokyo, Japan, 1970.
8. AKASHI, T., SUGANO, I., KENMOKU, Y., SHINMA, Y., and TSUJI, T. *Low-Loss and High-Stability Mn-Zn Ferrites* in Proceedings of the International Conference, ed., Y. Hoshino, S. Iida, and M. Sugimoto, University Park Press, Tokyo, Japan, 1970.